DEVELOPMENT OF SECONDARY CROSSFLOW INSTABILITY NEAR BREAKDOWN INTO TURBULENCE

Evelien van Bokhorst, Chris Atkin
City, University of London

Abstract

Throughout the years the transition process from laminar to turbulent flow has been studied in numerous experimental and numerical studies. Since for laminar flow the skin friction is lower compared to turbulent flow, the subject currently receives increased attention in the quest to design a laminar flow aeroplane. In the current study the transition process on a swept surface is studied with high resolution hot-wire scans. Up to now most studies focused on the development of the primary instability and the first growth stages of the secondary instability. Here the focus is on the structure of the secondary crossflow instability from its origin to breakdown. It has been found that, in the early growth stages, the characteristics of the structure agree well with previous studies. Close to breakdown of the flow the main structure divides up into smaller structures which are thought to be due to a developing turbulent wedge.

1 Introduction and background

Transition from laminar to turbulent flow on a swept wing with a favourable pressure gradient is dominated by the crossflow instability. When environmental disturbances such as roughness or free-stream turbulence are small the transition path consists of the following steps. In the receptivity stage the small disturbances from the environment interact with the boundary layer and perturbations are created close to the neutral stability point. The stationary crossflow vortices then grow first in a linear and then in a non-linear manner until the mean velocity profiles are inflected and a secondary instability appears. This instability is a high frequency travelling wave and grows explosively, after which the flow breaks down into turbulence. The receptivity and growth of the primary crossflow instability have been studied by several computational and experimental investigations [1, 2]. The characteristics of the secondary instability have been studied experimentally by forcing by means of blowing and suction at the wall [3, 4, 5]. In these studies the structure of the secondary instability looks similar and consists of vortex structures whose vortex axis is tilted with respect to the primary crossflow axis. The forcing allows the phase and structure of the secondary instability to be obtain. The first stages of the growth of this instability on a swept wing have been investigated in these studies, however the later development and breakdown into turbulence have not been studied in detail.

In depth knowledge about the origin and development of the secondary instability could be of use in transition prediction methods, which often only take into account the linear growth phase of the primary instability (e.g. the e^N method [6, 7]).

In the current study the focus is on visualizing the secondary instability at different stages of its development. It is thought that this data could be used to compare to the flow structures obtained from computational studies.

2 Experimental set-up and instrumentation

The experiments were carried out at the UK National Low Turbulence facility at City, University of London. This facility has low freestream turbulence levels (<0.01% up to 20m/s bandpass filtered from 2Hz-10kHz) which

makes it an excellent facility to study the transition process dominated by the stationary crossflow instability.

The experimental model consisted of a 45 degrees swept flat plate with two displacement bodies (DB) which create the favourable pressure gradient on the plate (Fig. 1). A single hot-wire was aligned with the x-axis such that the streamwise velocity component could be measured. The hot-wire was mounted to a traverse which had a step size of about 10μm in the x,y and z-directions. This set-up offered the high spatial and temporal resolution which is necessary to study the development of the crossflow instability in detail.

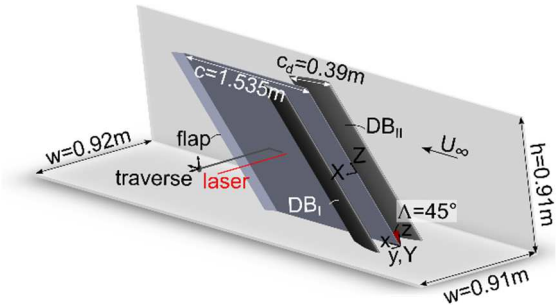

Fig. 1: Experimental set-up.

Having first established the necessary conditions for the secondary instability in the absence of forcing, the flow is then excited through a 0.5mm hole in the plate, close to the onset of the instability (Fig 2). At the back of the plate a small speaker is attached; the frequency and amplitude of excitation are controlled using a LABVIEW interface. The excitation frequency was chosen by analyzing the frequency content of the time signals where the natural secondary instability appears. Even though the secondary instability is a vortical structure with three velocity components, previous studies have shown that the main structure can be well captured with a single hot-wire [3, 4, 5].

The hot-wire signal was filtered with a bandpass filter (2-10 kHz) such that the fluctuating velocity component u'_{rms} could be determined. The phase between the filtered hot-wire signal and excitation signal was obtained by calculating the cross-spectral density. With this phase a time shift was calculated and applied to the filtered hot-wire signal. Applying this shift ensured that all the time signals started at the same phase such that the phase-averaged velocity, u_{ph}, could be obtained.

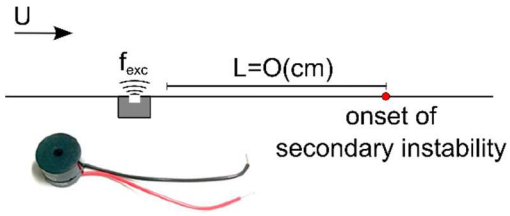

Fig 2: Excitation mechanism of the secondary instability.

3 Results and discussion

3.1 Early development of the secondary instability

First the results of the current study are compared to previous studies in terms of structure, length-scales, orientation and velocities. In Fig. 3 the streamwise velocity field is shown for different x/c locations.

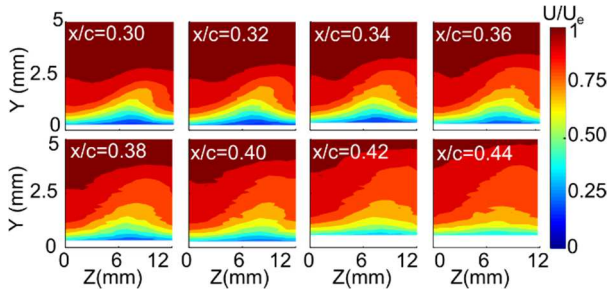

Fig. 3: Streamwise mean velocity fields at different x/c locations.

It is shown that a stationary vortex is growing and breaking down. From the power spectra of the bandpass-filtered hot-wire signal it was found that the secondary instability starts to grow from x/c = 0.32 in a frequency band from 0.8 kHz – 3 kHz (Fig. 4). From this an excitation frequency of 2 kHz was chosen.

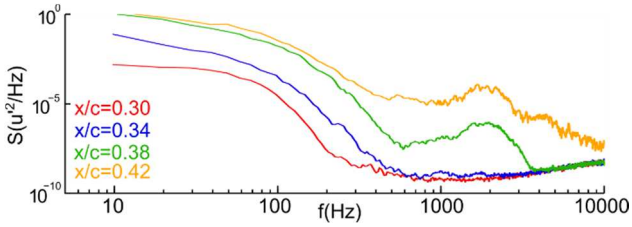

Fig. 4:Power spectra of fluctuating velocity at different streamwise locations.

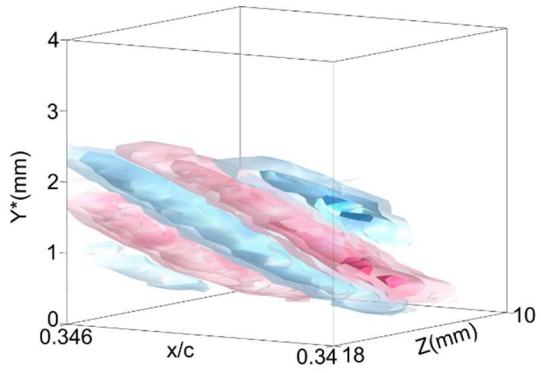

Fig. 5: Phase averaged velocity distribution of the secondary instability at x/c=0.34.

In Fig. 5 the phase-averaged velocity distribution at 2 kHz is shown at x/c = 0.34. The patches of alternating positive and negative velocity resemble the structure found in previous experimental and computational studies [3, 4, 5, 6]. In Fig. 6 the phase-averaged velocity distribution in the x_sY-plane is shown. (The x_s coordinate is the streamline coordinate which is found by tracking the middle of the stationary vortex, usingh the data from Fig. 3). From the streamwise structures, a wavelength of 7.48mm was found and a corresponding phase velocity of $0.74U_\infty$. This is very similar to the values found of $0.78U_e$ and $0.84U_\infty$ in previous studies [3, 5, 7]. Finally, the elevation angle, γ, is found which represents the angle between the x_s-axis and the secondary instability structure. An angle of 14 degrees was found which is in the range of angles 12 to 21 degrees found in [8] and [5] respectively.

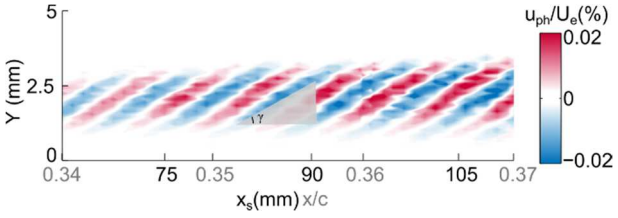

Fig. 6: Phase averaged velocity distribution in the x_sY-plane.

3.2 Non-linear development of the secondary instability

From the results of the early development of the secondary instability it was concluded the instability exhibited similar characteristics to the secondary instability found in previous studies. Next, the secondary instability in the later stages of the development was visualized in the x_sY, YZ and x_sZ-planes. In Fig. 6 the breakdown of a stationary vortex is shown in the x_sZ-plane. A wedge structure is apparent at $x_s \approx 130$mm. From this point the structure of the secondary instability becomes less coherent, indicating that the stationary vortex is breaking down. The wedge structure has been observed before in flow visualizations [9], hot-wire experiments [10] and computational studies [6], however, the structure of the secondary instability in the wedge has not been observed before.

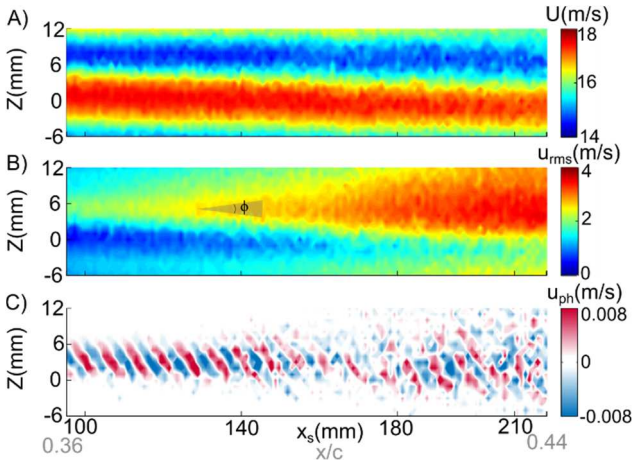

Fig. 7: Breakdown of a stationary crossflow vortex in the x_sZ-plane. A) Mean flow velocity. B) Fluctuating velocity component. C) Phase-averaged velocity.

The wedge spreading angle, ϕ, as indicated in Fig. 7B, was determined from three different wedge structures. An angle of 8 degrees was found with a standard deviation of 0.4 degrees. Previous studies did not report wedge angles, however, from the Figures presented in [6] an angle of 10 degrees was estimated. These angles are similar to the spreading angles of turbulent spots and turbulent wedges caused by large roughness protrusions [11], suggesting that the physics of the spreading mechanism is similar for all these cases.

In Fig. 8 the development is shown in the x_sY-plane. It is seen that the fluctuations become stronger from x/c = 0.34 to x/c = 0.4. After that the strength does not increase, which indicates that saturation and breakdown occurs. It is also seen that, even though the flow breaks down, the

orientation and wavelength of the secondary instability structure does not change significantly. Consequently, the phase-velocity also stays the same. In [4] the onset and breakdown of the secondary instability of a single vortex was measured and visualized with high spatial resolution. Initially, the structure is similar, however, going downstream the breakdown into smaller structures has not been observed. The reason for this is unclear, since when the flow becomes turbulent it would be expected that structures are broken up and a more chaotic flow appears.

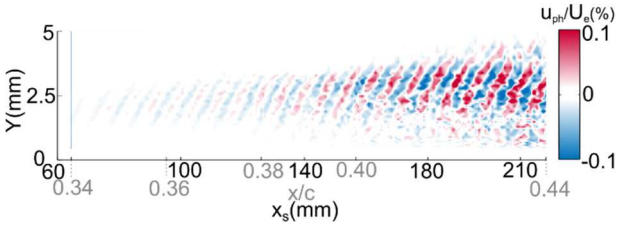

Fig. 8: Phase-averaged velocity distribution in the x_sY-plane.

In Fig. 9 the structure in the wall-normal and spanwise plane is shown at x/c = 0.34, 0.38 and 0.40. From x/c = 0.34 to x/c = 0.38 the phase-averaged velocity becomes stronger, as also observed in Fig. 7, and a slight spreading over the vortex is shown. At x/c = 0.40, which is in the middle of the wedge, the structure has spread over the entire vortex. Furthermore, the initial structure has broken down in smaller structures which are also shown in the three-dimensional representation. It seems that the structure has been torn apart in the spanwise direction due to the increased spanwise extent of the wedge. It is interesting that, even though the flow is breaking down, such a coherent structure could still be detected. In [6] the breakdown process of the secondary instability was calculated with a direct numerical simulation. The structures found in the present study at x/c = 0.4 could not be distinguished from numerical noise in their results which they explain as a limitation of the numerical method.

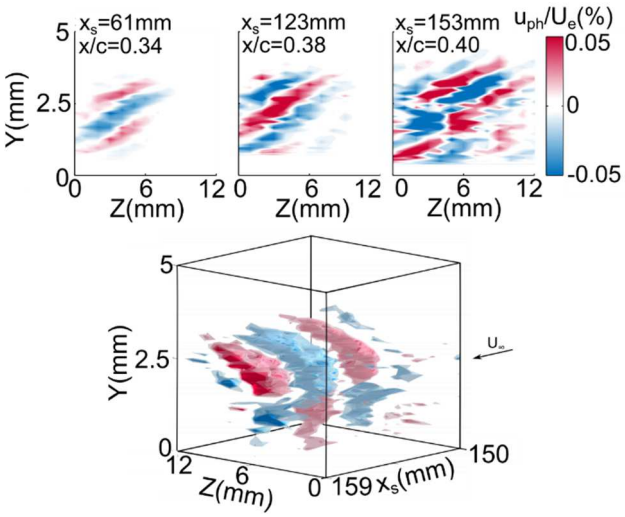

Fig. 9: Structure of the secondary instability at different x/c locations.

4 Conclusions

In this study the structure of the secondary instability in different development stages has been measured. With scans of the phase-averaged velocities in different planes the three-dimensional structure could be visualized. In the early development stages the characteristics of the secondary instability agree with those found in previous studies. Close to full transition into turbulence a wedge appears and the secondary instability structure breaks down into smaller parts. These structures have not been measured and visualized in previous studies and it is thought that in combination with computations the underlying physics can be better understood.

Acknowledgments

The authors acknowledge the support and technical expertise of Prof. Michael Gaster, without which this project would not be possible. Gratitude is also extended to Airbus, InnovateUK and ESPRC for funding this project under the ALFET and LFC-UK projects respectively.

References

[1] H. Bippes, "Basic experiments on transition in three-dimensional boundary layers dominated by crossflow instability," *Progress in Aerospace Sciences,* vol. 35, no. 12, pp. 363-412, 1999.

[2] W. Saric, H. Reed and E. White, "Stability and transition of three-dimensional boundary layers," *Annual review of fluid mechanics,* vol. 35, no. 1, pp. 413-440, 2003.

[3] M. Kawakami, Y. Kohama and M. Okutsu, "Stability characteristics of stationary crossflow vortices in three-dimensional boundary layer," in *37th Aerospace Sciences Meeting and Exhibit*, Reno, NV, 1999.

[4] V. Chernoray, A. Dovgal, V. Kozlov and L, "Experiments on secondary instability of streamwise vortices in a swept-wing boundary layer," *Journal of Fluid Mechanics,* vol. 534, pp. 295-325, 2005.

[5] J. Serpieri and M. Kotsonis, "Spatio-temporal characteristics of secondary instabilities in swept wing boundary layers," in *46th AIAA Fluid Dynamics Conference*, Washington D.C., 2016.

[6] P. Wassermann and M. Kloker, "Mechanisms and passive control of crossflow-vortex-induced transition in a three-dimensional boundary layer," *Journal of Fluid Mechanics,* vol. 456, pp. 49-84, 2002.

[7] M. Malik, F. Li, M. Choudhari and C. Chang, "Secondary instability of crossflow vortices and swept-wing boundary-layer transition," *Journal of fluid mechanics,* vol. 399, pp. 85-115, 1999.

[8] G. Bonfigli and M. Kloker, "Secondary instability of crossflow vortices: validation of the stability theory by direct numerical simulation," *Journal of fluid mechanics,* vol. 583, pp. 229-272, 2007.

[9] E. White and W. Saric, "Application of variable leading-edge roughness for transition control on swept wings.," in *38th Aerospace Sciences Meeting and Exhibit, Aerospace Sciences Meetings*, Reno, NV, 2000.

[10] V. Borodulin, A. Ivanov, Y. Kachanov and A. Roschektaev, "Receptivity coefficients at excitation of cross-flow waves by freestream vortices in the presence of surface roughness," *Journal of Fluid Mechanics,* vol. 716, pp. 487-527, 2017.

Contact Author Email Address

chris.atkin.1@city.ac.uk

Copyright Statement